Molecular Cell, Vol. 6, 931–937, October, 2000, Copyright ©2000 by Cell Press

Gene Repression by Coactivator Repulsion

Kate Senger,* Menie Merika,* Theodora Agalioti,* Junming Yie,* Carlos R. Escalante,† Guoying Chen,* Aneel K. Aggarwal,† and Dimitris Thanos*‡
*Department of Biochemistry and Molecular Biophysics
Columbia University
New York, New York 10032
†Structural Biology Program
Department of Physiology and Biophysics
Mount Sinai School of Medicine
New York, New York 10029

Summary

We show that the IRF-2 oncoprotein represses virus-induced IFN-β gene transcription via a novel mechanism. Virus infection induces recruitment of IRF-2 to some of the endogenous IFN-β enhancers as part of the enhanceosome. Enhanceosomes bearing IRF-2 cannot activate transcription, due to the presence of a domain in IRF-2 that prevents enhanceosome-dependent recruitment of the CBP-Pol II holoenzyme complex. As a consequence, IRF-2 incorporation into enhanceosomes restricts the number of IFN-β promoters directing transcription. Remarkably, deletion of the IRF-2 gene increases IFN-β expression by expanding the number of cells capable of inducing IFN-β gene transcription in response to virus infection.

Introduction

The IRF (interferon regulatory factor) family of transcription factors is comprised of ten distinct members which share sequence homology in an ~120 aa region responsible for sequence-specific DNA binding. The IRF DNA binding domain folds into a helix-turn-helix motif that latches onto DNA, such that a recognition helix selects a short GAAA core target sequence with an accompanying bending of the DNA axis toward the protein (Escalante et al., 1998; Fujii et al., 1999). The ten distinct members of the family (IRF-1, IRF-2, IRF-3, IRF-4/Pip/ISCAT, IRF-5, IRF-6, IRF-7, IRF-8/ICSBP, IRF-9/ISGF3γ, and the viral IRFs [vIRFs]) have been implicated in multiple biological processes such as antiviral response, cytokine signaling, cell growth regulation, and hematopoietic development (reviewed in Mamane et al., 1999). The distinct and nonoverlapping roles of each family member are thought to be the result of slightly different DNA binding specificities, patterns of expression and/or association with other regulators. The multiplicity and specificity of individual IRF proteins in selecting partners (e.g., ETS, other IRFs, STATs, and coactivators) is determined by sequences localized at their carboxyl terminus.

IRF-1 was the first member of the family to be isolated by virtue of its ability to bind and activate transcription from the IFN-β promoter (Miyamoto et al., 1988). The IRF-2 protein, which was identified by its homology to IRF-1, can antagonize IRF-1-mediated activation of the IFN-β promoter (Harada et al., 1989). IRF-1 and IRF-2 display almost indistinguishable DNA binding specificities, and both proteins are inducible by virus infection or IFN treatment. However, in contrast to IRF-1, which functions as an activator and tumor suppressor, IRF-2 has oncogenic potential and functions as a repressor of transcription (Taniguchi et al., 1997). Furthermore, virus infection induces proteolytic degradation of the carboxy-terminal region of some IRF-2 molecules, thus resulting in a protein (BFi) that bears only the IRF DNA binding domain (Cohen and Hiscott, 1992; Palombella and Maniatis, 1992; Whiteside et al., 1994). The mechanisms of action of IRF-2 and BFi have remained obscure, since some studies suggested that both proteins repress transcription by a steric interference mechanism (Whiteside et al., 1994; Nguyen et al., 1995), whereas other studies suggested that IRF-2 but not BFi bears a domain required for repression of transcription (Palombella and Maniatis, 1992; Yamamoto et al., 1994).

Inactivation of the IRF-2 gene in mice revealed that the lack of IRF-2 protein did not cause constitutive IFN (α or β) expression in the absence of virus infection, but upon viral infection the levels of IFN-β or IFN-α were ~3-fold higher in IRF2$^{-/-}$ cells than in wild-type cells, and in both cases no change in the kinetics of activation and postinduction repression of the IFN genes occurred (Matsuyama et al., 1993). These results imply that somehow IRF-2 restricts IFN expression during the period of virus infection. Transcriptional activation of the IFN-β gene requires the coordinate induction of three distinct sets of transcription factors (NF-κB, IRFs, and ATF-2/c-Jun) that with the help of the architectural HMG I(Y) protein bind cooperatively to the enhancer, assembling the enhanceosome (reviewed in Maniatis et al., 1998; Munshi et al., 1999). The enhanceosome activates transcription by recruiting the CBP/p300 coactivator that is associated with the Pol II holoenzyme complex (Kim et al., 1998; Merika et al., 1998; Yie et al., 1999). Therefore, a question arises as to the mechanism by which IRF-2 lowers the level of IFN-β gene induction. IRF-2 could function either by preventing enhanceosome assembly by competing for DNA binding with some of the IFN-β activators or by reducing the ability of the enhanceosome to activate transcription via an unknown mechanism.

Results and Discussion

To test whether IRF-2 can compete with IRF-1 for DNA binding, we mixed equal amounts of recombinant proteins and incubated them with the PRDI oligonucleotide (one IRF binding site) for increasing amounts of time. Figure 1A demonstrates that IRF-1 displaced IRF-2 from its binding site, but not vice versa, in a time-dependent manner. The experiment shown in Figure 1B shows that

‡To whom correspondence should be addressed (e-mail: dt73@columbia.edu).

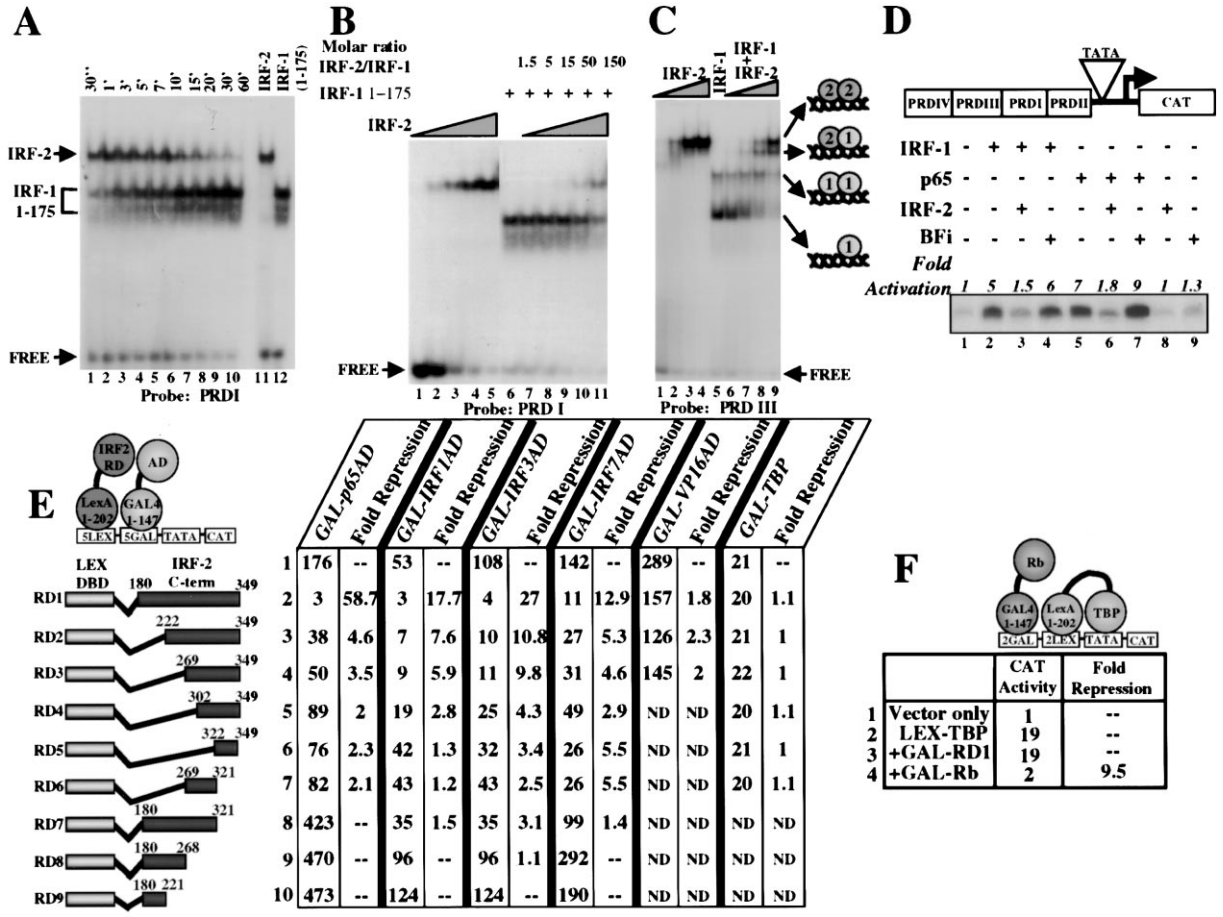

	GAL-p65AD	Fold Repression	GAL-IRF1AD	Fold Repression	GAL-IRF3AD	Fold Repression	GAL-IRF7AD	Fold Repression	GAL-VP16AD	Fold Repression	GAL-TBP	Fold Repression
1	176	--	53	--	108	--	142	--	289	--	21	--
2	3	58.7	3	17.7	4	27	11	12.9	157	1.8	20	1.1
3	38	4.6	7	7.6	10	10.8	27	5.3	126	2.3	21	1
4	50	3.5	9	5.9	11	9.8	31	4.6	145	2	22	1
5	89	2	19	2.8	25	4.3	49	2.9	ND	ND	20	1.1
6	76	2.3	42	1.3	32	3.4	26	5.5	ND	ND	21	1
7	82	2.1	43	1.2	43	2.5	26	5.5	ND	ND	20	1.1
8	423	--	35	1.5	35	3.1	99	1.4	ND	ND	ND	ND
9	470	--	96	--	96	1.1	292	--	ND	ND	ND	ND
10	473	--	124	--	124	--	190	--	ND	ND	ND	ND

		CAT Activity	Fold Repression
1	Vector only	1	--
2	LEX-TBP	19	--
3	+GAL-RD1	19	--
4	+GAL-Rb	2	9.5

Figure 1. IRF-2 Possesses a Domain that Represses Transcription in the Absence of Competitive DNA Binding

(A) An equimolar mixture of IRF-1(1–175) and IRF-2 was allowed to interact with the PRDI oligonucleotide for the times indicated at the top of the figure before EMSA analysis.

(B) A constant amount of IRF-1 (lane 6) was allowed to interact with the PRDI oligonucleotide for 60 min before the addition of increasing amounts of IRF-2. The molar ratio of IRF-2 over IRF-1 is depicted at the top of the figure.

(C) Shown is an EMSA experiment using the PRDIII oligonucleotide as a probe and increasing amounts of IRF-2 either alone (lanes 1–4) or with a constant amount of IRF-1 (lanes 6–9). Lane 5 depicts the amount of IRF-1 used. The identity of the protein-DNA complexes is illustrated on the right side of the gel.

(D) Shown is an in vitro transcription experiment using the IFN–β CAT as a template, HeLa nuclear extracts, and the combination of p65 or IRF-1 and IRF-2 or BFi depicted at the top of the figure. Correctly initiated mRNA was visualized by primer extension using a CAT primer.

(E) COS cells were transfected with the indicated LexA-IRF-2 expressing vectors (1 μg) along with vectors encoding GAL4-p65AD (100 ng), GAL4-IRF1AD (1 μg), GAL4-IRF3AD (1 μg), GAL4-IRF7AD (0.75 μg), GAL4-VP16 (200 ng), or GAL4-TBP (2 μg). Shown is the average of four independent experiments (15% variability).

(F) Same as in (E) but the reporter contained two GAL and LEX sites, the activator used was LEX-TBP (2 μg), and the repressors were GAL4-IRF-2(RD1) or GAL4-Rb (1 μg each)

IRF-2 can compete with IRF-1 for DNA binding (50% competition) but only at IRF-2/IRF-1 molar ratios that are greater than 150.

Since IRF-2 could not inhibit DNA binding of IRF-1, we tested whether it can form heterocomplexes with IRF-1 by performing EMSA experiments using the PRDIII element of the IFN-β enhancer (two IRF binding sites) as a probe. Figure 1C demonstrates that incubation of increasing amounts of IRF-2 (lanes 1–4) with a fixed amount of IRF-1 (lane 5) resulted in the formation of a novel complex that migrated with an intermediate mobility (lanes 6–9), thus implying assembly of an IRF-1/IRF-2 heterocomplex. Formation of this complex required both IRF sites, since it was not observed when PRDI (one IRF binding site) was used as a probe (Figures 1A and 1B). To test the transcriptional activity of the IRF-1/IRF-2 heterocomplex, we carried out in vitro transcription experiments using as template the IFN-β enhancer/promoter and HeLa nuclear extracts. Figure 1D shows that IRF-2 decreased IRF-1's transcriptional activity (compare lanes 2 and 3). Interestingly, substitution of full-length IRF-2 with a truncated version corresponding to BFi did not inhibit IRF-1's transcriptional activity (compare lanes 2 and 4). Similarly, IRF-2 but not BFi repressed NF-κB dependent transcriptional activation from the nearby PRDII element (Figure 1D, lanes 5–7). Thus, the carboxyl terminus of IRF-2 is required for repression of transcription activated by nearby IRF-1 and NF-κB molecules.

To identify the repression domain of IRF-2, we gener-

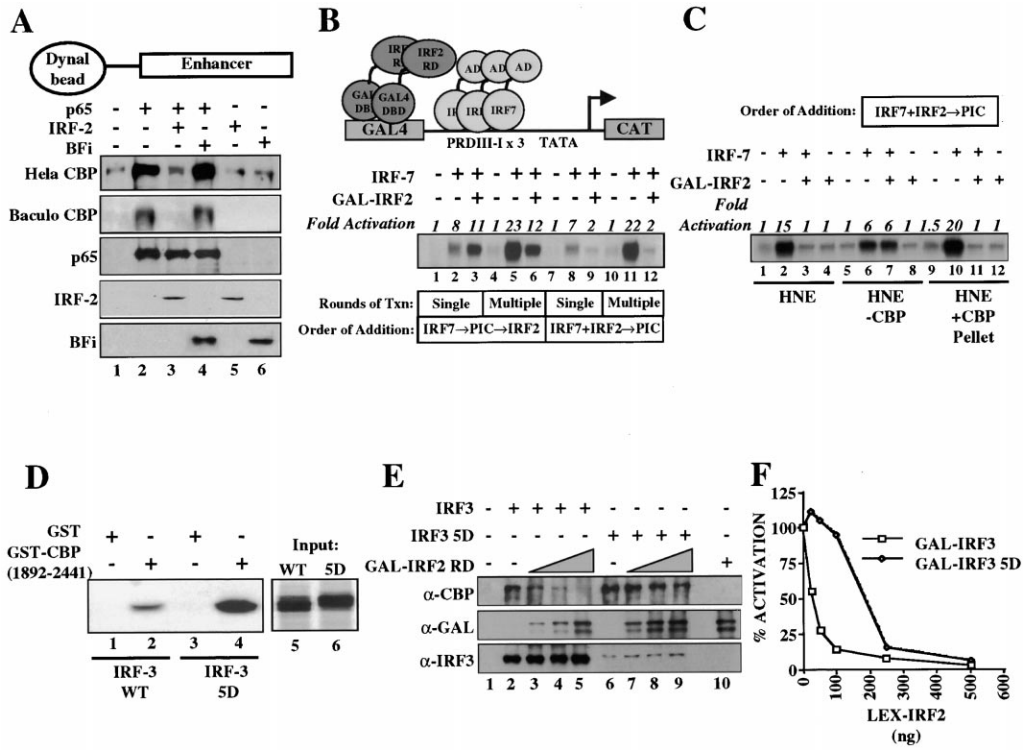

Figure 2. IRF-2 Represses Transcription by Inhibiting Recruitment of CBP by the IFN-β Gene Activators

(A) A biotinylated IFN-β enhancer oligonucleotide (−105 to −40) with or without p65 was coupled to magnetic Dynabeads and was incubated with 500 μg of HeLa nuclear extract (top panel) or 20 ng of baculovirus-expressed and purified CBP (second panel). The bound proteins were detected by Western blotting using CBP and p65-specific antibodies. The last three panels depict binding of p65, IRF-2, or BFi to the enhancer, respectively.

(B) Shown is an in vitro transcription experiment using a plasmid bearing one GAL4 site placed upstream of three copies of the PRDIII-I element as template (100 ng), HeLa nuclear extract and recombinant IRF-7 (200 ng), and GAL4-IRF-2 RD (500 ng). In lanes 1–6, IRF-7 was allowed to promote PIC assembly and then GAL4-IRF-2 RD was added. In lanes 7–12, IRF-7 and GAL4-IRF-2 RD were added together to the template followed by the addition of HNE.

(C) Same as in (B) except that either complete (lanes 1–4) or CBP-depleted (lanes 5–12) HeLa nuclear extract was used. In lanes 9–12, the CBP-depleted extract was supplemented by adding back the CBP immunoprecipitate.

(D) Shown is a GST pulldown experiment using radiolabeled WT IRF-3 (lanes 1 and 2) or IRF-3(5D) (lanes 3 and 4) and GST-CBP(1892–2441).

(E) The DNA template of Figure 2B was biotinylated and incubated with 500 ng of IRF-3 WT (lanes 2–5) or 25 ng of IRF-3(5D) (lanes 6–9) in the presence or the absence of increasing amounts of GAL4-IRF-2 RD. Next, the DNA-protein complexes were incubated with HNE, washed, and the bound proteins were detected by Western blotting.

(F) COS cells were cotransfected with the LexA-GAL4 reporter plasmid (300 ng) along with expression vectors for Lex-IRF-2 (RD1) (25 ng, 50 ng, 100 ng, 250 ng, and 500 ng) and GAL4-IRF-3(WT) or GAL4-IRF-3(5D) (1 μg each). Shown is one of two independent experiments (15% variability).

ated LexA-fused deletions of its C terminus that were tested for their ability to repress GAL4-based activators from a reporter bearing five LEX and five GAL4 sites after cotransfection in COS cells. Figure 1E shows that LEX-IRF-2(180–349) (RD1) strongly repressed GAL4-p65-, GAL4-IRF-1-, GAL4-IRF-3-, and GAL4-IRF-7-activated transcription (compare lines 1 and 2). However, N-terminal serial deletions to amino acid 302 (RD1–RD4) gradually relieved repression (lines 3–5). Removal of the carboxy-terminal 28 aa (RD7) dramatically reduced IRF-2-mediated repression (line 8). However, this region on its own is a weak repressing domain (RD5, line 6). Western blotting revealed that all LexA-IRF-2 fusion proteins were expressed at similar levels after transfection (data not shown). IRF-2 only weakly (2-fold) repressed transcription from GAL4-VP16 (Figure 1E) or from full-length GAL4 or from GAL4-Sp1 (not shown).

To test whether IRF-2 represses transcription by directly inhibiting assembly of the basal transcriptional machinery on the promoter, we carried out activator bypass experiments in which COS cells were transfected with a vector expressing a GAL4-TBP fusion in the presence or the absence of LEX-IRF2RD. Figure 1E (line 2) shows that GAL4-TBP stimulates transcription 21-fold in the absence of an activation domain and that coexpression of LEX-IRF-2RD fusion proteins did not affect GAL4-TBP-dependent transcription (lines 1–7). However, another repressor, the retinoblastoma protein Rb, which functions by recruiting histone deacetylases (Brehm et al., 1998; Magnaghi-Jaulin et al., 1998) and by directly preventing assembly of preinitiation complexes (Ross et al., 1999), strongly inhibited TBP-mediated activation of transcription (Figure 1F), a result consistent with previous experiments (De Luca et al., 1998). Thus, IRF-2 represses transcription neither by competitive DNA binding nor by inhibiting assembly of the basal transcriptional machinery directly or indirectly.

IRF-1, IRF-3, IRF-7, and p65 activate transcription by

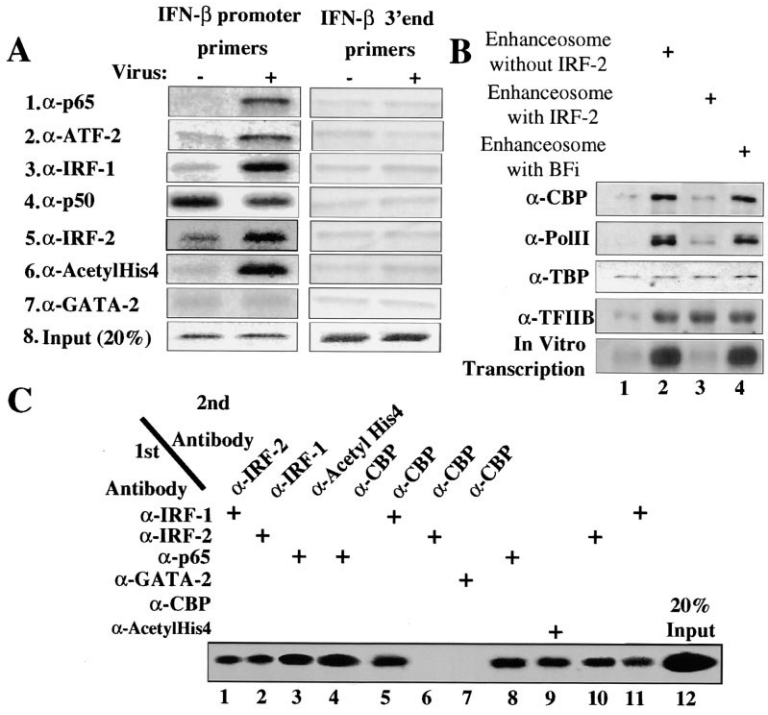

Figure 3. Incorporation of IRF-2 into the IFN-β Enhanceosome In Vivo or In Vitro Blocks CBP Recruitment

(A) HeLa cells were mock or virus infected for 6 hr and treated with formaldehyde to cross-link proteins bound to DNA. Soluble chromatin was immunoprecipitated with the indicated antibodies and analyzed by quantitative PCR using primers corresponding to either the promoter or the 3′ untranslated (as a control) region of the IFN-β gene.

(B) Enhanceosomes containing IRF-2 (lane 3) or BFi (lane 4) were assembled on a biotinylated IFN-β enhancer/promoter coupled to magnetic Dynabeads and were incubated with 500 μg of HeLa nuclear extract. The bound proteins were detected by Western blotting using CBP-, Pol II-, TBP-, or TFIIB-specific antibodies. The bottom panel of the figure shows an in vitro transcription experiment using the same template and combination of factors.

(C) Cross-linked chromatin prepared from virus-induced HeLa cells was immunoprecipitated with the indicated antibodies (left column). The immune complexes were extensively washed, eluted, and reprecipitated using the antibodies indicated on the top part of the gel and finally analyzed by quantitative PCR using the IFN-β promoter primers (lanes 1–7). Lanes 8–11 show single immunoprecipitations used as a positive control.

recruiting the CBP/p300 coactivator (Maniatis et al., 1998; Munshi et al., 1999). This observation, taken together with our demonstration that IRF-2 cannot directly inhibit assembly of the basal machinery, led us to examine whether IRF-2 represses the aforementioned activators by preventing them from recruiting CBP. Recombinant p65, IRF-2, or BFi and combinations thereof were allowed to bind to a biotinylated IFN-β enhancer oligonucleotide immobilized on streptavidin magnetic beads, followed by incubation with HeLa nuclear extracts (HNE) and Western blotting to identify bound proteins (Yie et al., 1999). Figure 2A (top panel) shows that p65 efficiently recruits CBP from the nuclear extract to the enhancer (compare lanes 1 and 2), and this recruitment was prevented by full-length IRF-2 but not BFi (compare lane 2 with lanes 3 and 4). Importantly, a similar result was obtained when recombinant baculovirus–expressed and purified CBP was used instead of the HNE (Figure 2A, second panel), thus implying that the effect of IRF-2 on CBP recruitment is not mediated by other proteins in the extract.

To test whether inhibition of CBP recruitment by IRF-2 results in blockage of functional preinitiation complex (PIC) assembly, we carried out in vitro transcription experiments in which IRF-2 was added before or after PIC assembly and allowed single or multiple rounds of transcriptional initiation. Figure 2B shows that under single round transcription, IRF-7 activates transcription 8-fold (compare lanes 1 and 2). Addition of GAL4-IRF-2RD after the formation of PICs did not inhibit IRF-7's ability to stimulate transcription (compare lanes 2 and 3). In contrast, addition of GAL4-IRF-2RD before PIC assembly (together with IRF-7) significantly reduced the ability of IRF-7 to promote functional PIC assembly (compare lanes 8 and 9). Remarkably, when multiple rounds of transcription were allowed, addition of IRF-2 after the assembly of the first functional PICs inhibited only the subsequent rounds of transcription reinitiation (compare lanes 5 and 6), whereas the presence of IRF-2 before the first PIC assembly resulted in almost complete repression of transcription (compare lanes 11 and 12). Similar results were obtained when NF-κB was used instead of IRF-7 (data not shown).

To examine whether IRF-2 blocks transcription in vitro by prohibiting the activators from recruiting CBP, we carried out in vitro transcription experiments using HeLa nuclear extracts in which CBP/p300 had been immunodepleted. Under our conditions, more than 95% of CBP/p300 is depleted (Yie et al., 1999). Figure 2C shows that in the CBP-depleted extracts, IRF-7 stimulated transcription 2.5-fold less efficiently than in the mock-depleted extracts (compare lanes 2 and 6). Significantly, IRF-2 did not repress transcription activated by IRF-7 in the CBP-depleted extracts (compare lanes 6 and 7). Depletion of CBP from the extracts is responsible for the inability of IRF-2 to repress transcription because adding back the CBP immunoprecipitate restored repression (lanes 9–12). These experiments strongly suggest that IRF-2 represses transcription by inhibiting recruitment of CBP by activators.

A key prediction of the above results is that the efficiency by which IRF-2 represses a given activator would be inversely proportional to the strength by which that activator interacts with CBP. To this end, we measured the efficiency by which IRF-2 represses transcription activated by wild-type IRF-3 and IRF-3(5D). The latter bears five aspartic acids in place of five serines, which results in higher transcriptional activation (Mamane et

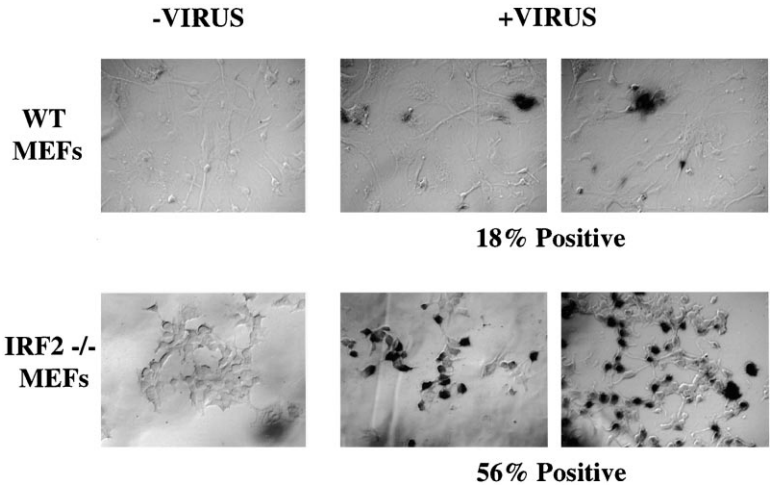

Figure 4. Inactivation of the IRF-2 Gene Causes an Increase in the Percentage of IFN-β Producing Cells in Response to Virus Infection

Mouse embryonic fibroblasts derived from wild-type or from IRF-2$^{-/-}$ mice were mock or virus infected for 12 hr, fixed, and hybridized with a digoxigenin-labeled IFN-β antisense RNA probe. IFN-β-producing cells were identified using a digoxigenin-specific antibody. Shown is one of two independent experiments. In the other experiment, the percentage of IFN-β producing wild-type and IRF-2$^{-/-}$ cells was 16% and 46%, respectively.

al., 1999) due to its higher affinity for CBP (Figure 2D). As seen in Figure 2E, wild-type IRF-3 recruits CBP (lane 2), and this recruitment is strongly reduced by GAL-IRF-2 (compare lane 2 with lanes 3–5). Since IRF-3(5D) interacts with CBP stronger than IRF-3 WT, we used 20 times less IRF-3(5D) to ensure that approximately equal amounts of CBP were recruited by both proteins. As predicted, IRF-2 only weakly inhibited recruitment of CBP by IRF-3(5D) (compare lane 6 with lanes 7–9). Consistent with the above, IRF-2 inhibited IRF-3(5D)-dependent transcription in vivo ~5 times weaker than it inhibited wild-type IRF-3 (Figure 2F).

The experiments described so far suggest that IRF-2 exerts its repressing activity by inhibiting nearby activators from recruiting CBP. Therefore, we investigated whether IRF-2 could assemble on endogenous IFN-β enhanceosomes in conjunction with the IFN-β gene activators by carrying out chromatin immunoprecipitation experiments. Figure 3A shows that p65, ATF-2, and IRF-1 bind to the IFN-β enhancer in vivo in a virus-inducible manner. Remarkably, we found that in addition to the aforementioned activators, the IRF-2 repressor is also recruited into enhanceosomes in response to virus infection (Figure 3A). The amount of IFN-β promoter DNA amplified from p50 immunoprecipitates prepared from induced cells was approximately half of that obtained from uninduced cells, a result consistent with the presence of p50 homodimers and p50/p65 heterodimers on the IFN-β enhancer in uninduced and induced cells, respectively. This is consistent with the notion that p50 homodimers are involved in preinduction repression, whereas the p50/p65 heterodimer is involved in activation of IFN-β gene transcription (Maniatis et al., 1998; Munshi et al., 1999).

To test whether IRF-2's role in the IFN-β enhanceosome is indeed the inhibition of CBP recruitment, we carried out in vitro recruitment and transcription experiments using the IFN-β enhancer immobilized on streptavidin magnetic beads. Figure 3B shows that incorporation of IRF-2 into IFN-β enhanceosomes blocks recruitment of CBP and the associated RNA Pol II (compare lanes 2 and 3, top and second panel) and strongly inhibits activation of transcription (bottom panel). As a control, we showed that constitutive binding of TBP and recruitment of TFIIB to the enhancer (Kim et al., 1998; Yie et al., 1999) are not affected by IRF-2 (Figure 3B, third and fourth panels). The latter observation is consistent with our previous experiments demonstrating that recruitment of TFIIB and binding of TBP to the promoter occur independently of the CBP-Pol II holoenzyme (Yie et al., 1999), at least on naked DNA templates.

To determine whether IRF-1 and IRF-2 could indeed coexist within the same enhanceosomes in vivo, we performed sequential chromatin immunoprecipitation experiments (Figure 3C). Formaldehyde cross-linked chromatin fragments prepared from virus-infected HeLa cells were immunoprecipitated using IRF-1 (lane 1), IRF-2 (lane 2), and p65 (lane 3) specific antibodies. The immune complexes were extensively washed; the chromatin was eluted and reprecipitated with antibodies against IRF-2, IRF-1, and histone H4 acetyl-lysine (lanes 1–3, respectively). As seen in Figure 3C (lanes 1 and 2), IRF-1 and IRF-2 coexist in the same enhanceosomes. Whether the enhanceosome-bound IRF-2 blocks recruitment of CBP was investigated by using antibodies against IRF-2, IRF-1, or p65 for the first round of immunoprecipitation followed by reprecipitation using CBP-specific antibodies. Figure 3C shows that p65- or IRF-1-containing enhanceosomes recruit CBP (lanes 4 and 5, respectively). In sharp contrast, IRF-2-containing enhanceosomes do not recruit CBP (lane 6), a result consistent with our previous experiments. In summary, these studies strongly suggest that following virus infection, some enhanceosomes cannot recruit CBP because they contain IRF-2.

An unusual characteristic of IFN-α or -β expression is that even under optimal conditions of virus infection, only 10%–40% of cells induce these genes (Zawatzky et al., 1985; Enoch et al., 1986). This heterogeneity is not due to mixed populations of producing and nonproducing cells in the culture but rather is a stochastic phenomenon, as revealed by cell cloning experiments (Zawatzky et al., 1985). Our demonstration that IRF-2 is incorporated into enhanceosomes that are transcriptionally inactive in vivo prompted us to examine whether there is an increase of IFN-β-producing cells in the absence of IRF-2. Mouse embryonic fibroblasts derived from wild-type mice or mice lacking the IRF-2 gene were

infected with Sendai virus for 12 hr and then hybridized with an antisense IFN-β digoxigenin-labeled RNA probe. Figure 4 shows that only a small fraction of wild-type cells transcribe the IFN-β gene in response to virus infection. Remarkably, the percentage of IFN-β-producing cells is three times higher in mouse embryonic fibroblasts lacking the IRF-2 gene. Thus, the lack of IRF-2 increases the number of cells inducing the IFN-β gene.

We demonstrated that IRF-2 represses transcription via a novel mechanism; that is, by preventing recruitment of the CBP/p300 coactivator and the associated RNA Pol II holoenzyme complex to promoters. That inhibition of CBP recruitment can be recapitulated with recombinant proteins implies that this inhibition is not mediated by another protein recruited by IRF-2 but rather by the IRF-2 repression domain itself. We have shown that the repression domain of IRF-2 does not interact with either the activators or CBP (data not shown), yet it blocks recruitment of CBP. Furthermore, IRF-2-mediated repression can be counteracted by either increasing the negative charges in activation domains, thereby strengthening activator-CBP interactions, or by decreasing the basic character of IRF-2's repression domain (Yamamoto et al., 1994). We propose that basic amino acids in the repression domain build a positively charged microenvironment that repels incoming CBP or destabilizes the CBP–activator interaction in the absence of any detectable repression domain–activator or repression domain–CBP interactions. Consistent with this model is our demonstration that IRF-2 cannot repress transcription when positioned further upstream from the activators or outside of the enhanceosome context, thus indicating that its proximity to the activator-CBP interface is critical for function (data not shown).

A remarkable feature of IRF-2's function is that it works like a "Trojan horse" to repress transcription by invading some enhanceosomes. IRF-2 "sneaks in" along with the IFN-β gene activators to some enhancers, forms enhanceosomes, and converts these enhanceosomes into transcriptionally silent complexes by preventing them from recruiting CBP. It appears that the stochastic assembly of IRF-2 into IFN-β enhanceosomes in vivo inversely correlates with the chance of a given cell to induce the IFN-β gene, as revealed by the analysis of IFN-β gene expression in individual cells derived from wild-type and IRF-2$^{-/-}$ mice. We found that in the absence of IRF-2, a larger proportion of cells are capable of inducing the IFN-β gene when compared to wild-type cells, thus indicating a larger number of transcriptionally active enhanceosomes.

Experimental Procedures

Electrophoretic Mobility Shift Assays, In Vitro Transcription, and Cell Transfection

Electrophoretic mobility shift assay (EMSA) experiments, protein expression, and cell transfections were performed as previously described (Merika et al., 1998). In vitro transcription reactions in complete and CBP/p300–depleted extracts were carried out as described before (Yie et al., 1999). Immobilization of the IFN-β enhancer to Dynabeads and recruitment of CBP were carried out as previously described (Yie et al., 1999).

In Situ Hybridization

Mouse IFN-β antisense RNA was synthesized using SP6 polymerase and digoxigenin-labeled nucleotides. MEFs were cultured on 12 mm diameter BIOCOAT poly-L-lysine coated coverslips (Fischer) and either mock or virus infected for 12 hr, washed once with PBS, and fixed with 4% paraformaldehyde in 1× PBS. Hybridization, washes, and staining were carried out as previously described (Schaeren-Wiemers and Gerfin-Moser, 1993).

Chromatin Immunoprecipitation Assays

Chromatin immunoprecipitations were carried out as described previously (Parekh and Maniatis, 1999) using 10 μg of antibodies against p65, ATF-2, IRF-1, p50, IRF-2, acetylated H4, and GATA-2. For the sequential chromatin immunoprecipitation assay, the reactions were scaled up 5-fold. PCR reactions were performed in 50 μl volume with 20 μl of immunoprecipitated material, 0.5 μg of each primer set, 2.5 U of Taq DNA polymerase (Boehringer Mannheim) in a buffer supplied by the manufacturer.

Acknowledgments

We thank S. J. Weintraub, Y. Chang, P. Moore, J. Hiscott, S. Chellappan, V. Palombella, and T. Maniatis for reagents used in this study. We thank B. Dynlacht, J. Falvo, and B. Parekh for their advice on the chromatin immunoprecipitation experiments. We also thank Tom Maniatis, Richard Mann, and Nikhil Munshi for critical reading of the manuscript and Tada Taniguchi for helpful discussions. This work was supported by grants from the National Institute of Health (1RO1GM54605), the Pew Scholars Program in Biomedical Sciences, the March of Dimes, the Irma T. Hirschl Foundation (to D. T.), and from National Institute of Health (1RO1AI41706) to A. K. A. and D. T.

Received April 10, 2000; revised July 31, 2000.

References

Brehm, A., Miska, E.A., McCance, D.J., Reid, J.L., Bannister, A.J., and Kouzarides, T. (1998). Retinoblastoma protein recruits histone deacetylase to repress transcription. Nature *391*, 597–601.

Cohen, L., and Hiscott, J. (1992). Characterization of TH3, an induction specific protein interacting with the interferon-β promoter. Virology *191*, 589–599.

De Luca, P., Majello, B., and Lania, L. (1998). Retinoblastoma protein tethered to promoter DNA represses TBP-mediated transcription. J. Cell. Biochem. *70*, 281–287.

Enoch, T., Zinn, K., and Maniatis, T. (1986). Activation of the human β−interferon gene requires an interferon-inducible factor. Mol. Cell. Biol. *6*, 801–810.

Escalante, C.R., Yie, J., Thanos, D., and Aggarwal, A.K. (1998). Structure of IRF-1 with bound DNA reveals determinants of interferon regulation. Nature *391*, 103–106.

Fujii, Y., Shimizu, T., Kusumoto, M., Kyogoku, Y., Taniguchi, T., and Hakoshima, T. (1999). Crystal structure of an IRF-DNA complex reveals novel DNA recognition and cooperative binding to a tandem repeat of core sequences. EMBO J. *18*, 5028–5041.

Harada, H., Fujita, T., Miyamoto, M., Kimura, Y., Maruyama, M., Furia, A., Miyata, T., and Taniguchi, T. (1989). Structurally similar but functionally distinct factors, IRF-1 and IRF-2, bind to the same regulatory elements of IRF and IRF-inducible genes. Cell *58*, 729–739.

Kim, T.K., Kim, T.H., and Maniatis, T. (1998). Efficient recruitment of TFIIB and CBP-RNA polymerase II holoenzyme by an interferon-β enhanceosome in vitro. Proc. Natl. Acad. Sci. USA *95*, 12191–12195.

Magnaghi-Jaulin, L., Groisman, R., Naguibneva, I., Robin, P., Lorain, S., Le Villain, J.P., Troalen, F., Trouche, D., and Harel-Bellan, A. (1998). Retinoblastoma protein represses transcription by recruiting histone deacetylase. Nature *391*, 601–605.

Mamane, Y., Heylbroeck, C., Genin, P., Algarte, M., Servant, M.J., LePage, C., DeLuca, C., Kwon, H., Lin, R., and Hiscott, J. (1999). Interferon regulatory factors: the next generation. Gene *237*, 1–14.

Maniatis, T., Falvo, J.V., Kim, T.H., Kim, T.K., Lin, C.H., Parekh, B.S., and Wathelet, M.G. (1998). Structure and function of the interferon-beta enhanceosome. Cold Spring Harbor Symp. Quant. Biol. *63*, 609–620.

Matsuyama, T., Kimura, T., Kitagawa, M., Pfeffer, K., Kawakami, T., Watanabe, N., Kondig, T.M., Amakawa, R., Kishihara, T., Wakeham, A., et al. (1993). Targeted disruption of IRF-1 or IRF-2 results in abnormal type I IFN gene induction and aberrant lymphocyte development. Cell *75*, 83–97.

Merika, M., Williams, A.J., Chen, G., Collins, T., and Thanos, D. (1998). Recruitment of CBP/p300 by the IFN beta enhanceosome is required for synergistic activation of transcription. Mol. Cell *1*, 277–287.

Miyamoto, M., Fujita, T., Kimura, Y., Maruyama, M., Harada, H., Sudo, Y., Migata, T., and Taniguchi, T. (1988). Regulated expression of a gene encoding a nuclear factor, IRF-1, that specifically binds to the IFN-β gene regulatory elements. Cell *54*, 903–913.

Munshi, N., Yie, J., Merika, M., Senger, K., Lomvardas, S., Agalioti, T., and Thanos, D. (1999). The IFN-β enhancer: a paradigm for understanding activation and repression of inducible gene expression. Cold Spring Harbor Symp. Quant. Biol. *64*, 149–159.

Nguyen, H., Mustafa, A., Hiscott, J., and Lin, R. (1995). Transcription factor IRF-2 exerts its oncogenic phenotype through the DNA binding/transcription repression domain. Oncogene *11*, 537–544.

Palombella, V., and Maniatis, T. (1992). Inducible processing of interferon regulatory factor-2. Mol. Cell. Biol. *12*, 3325–3336.

Parekh, B.S., and Maniatis, T. (1999). Virus infection leads to localized hyperacetylation of histones H3 and H4 at the IFN-β promoter. Mol. Cell *3*, 125–129.

Ross, J.F., Liu, X., and Dynlacht, B.D. (1999). Mechanism of transcriptional repression of E2F by the retinoblastoma tumor suppressor protein. Mol. Cell *3*, 195–205.

Schaeren-Wiemers, N., and Gerfin-Moser, A. (1993). A single protocol to detect transcripts of various types and expression levels in neural tissue and cultured cells: in situ hybridization using digoxigenin-labelled cRNA probes. Histochemistry *100*, 431–440.

Taniguchi, T., Lamphier, M.S., and Tanaka, N. (1997). IRF-1: the transcription factor linking the interferon response and oncogenesis. Biochim. Biophys. Acta Rev. Cancer *1333*, M9–M17.

Whiteside, S.T., King, P., and Goodbourn, S. (1994). A truncated form of the IRF-2 transcription factor has the properties of a postinduction repressor of interferon-β gene expression. J. Biol. Chem. *269*, 27059–27065.

Yamamoto, H., Lamphier, M.S., Fujita, T., Taniguchi, T., and Harada, H. (1994). The oncogenic transcription factor IRF-2 possesses a transcriptional repression and a latent activation domain. Oncogene *9*, 1423–1428.

Yie, J., Senger, K., and Thanos, D. (1999). Mechanism by which the IFN-β enhanceosome activates transcription. Proc. Natl. Acad. Sci. USA *96*, 13108–13113.

Zawatzky, R., De Maeyer, E., and De Maeyer-Guignard, J. (1985). Identification of individual interferon-producing cells by in situ hybridization. Proc. Natl. Acad. Sci. USA *82*, 1136–1140.